

Neutron scattering and μ SR studies on a Kondo lattice heavy fermion CeRuSn₃

V K Anand^{1,2}, D T Adroja^{1,3}, A Bhattacharyya^{1,3}, A D Hillier¹,
D Britz³, A M Strydom³, J W Taylor¹, A Fraile¹ and W Kockelman¹

¹ISIS Facility, Rutherford Appleton Laboratory, Chilton, Didcot, Oxon, OX11 0QX, United Kingdom

²Helmholtz-Zentrum Berlin für Materialien und Energie, Hahn-Meitner Platz 1, D-14109 Berlin, Germany

³Highly Correlated Matter Research Group, Physics Department, University of Johannesburg, P.O. Box 524, Auckland Park 2006, South Africa

E-mail: vivekkranand@gmail.com, devashibhai.adroja@stfc.ac.uk

Abstract. Kondo lattice heavy fermion system CeRuSn₃ exhibits anomalies in magnetic susceptibility and specific heat at a temperature $T \approx 0.6$ K (much lower than the average Kondo temperature $T_K \approx 3.1$ K) which are thought to be related to antiferromagnetic ordering or spin-glass transition. Our muon spin relaxation (μ SR) data show no clear evidence of long range magnetic order in CeRuSn₃ down to 84 mK. However, it reveals a slowing down of spin fluctuations below 0.6 K, and a glassy spin-dynamics seems more appropriate. The inelastic neutron scattering data reveal broad excitations around 6–8 meV due to the crystal field effect.

1. Introduction

The heavy-fermion compounds that belong to the large class of strongly correlated electronic systems present very rich physics due to its proximity to a quantum critical point (QCP) and have been a topic of intense research for last few decades [1–6]. Ce-based heavy fermion systems present fascinating physics due to the Kondo effect that competes with and becomes comparable to RKKY interaction in the vicinity of a QCP. Kondo lattice-heavy fermion CeRuSn₃ is an interesting example. CeRuSn₃ forms in LaRuSn₃-type cubic structure (space group $Pm\bar{3}n$, No. 223) in which Ce atoms occupy two different crystallographic sites, Ru and Sn atoms form trigonal RuSn₆ prisms, and the three-dimensional network of these prisms form cages which are occupied by Ce atoms [7]. An enhanced Sommerfeld coefficient γ together with a logarithmic increase ($-\ln T$ behavior) in resistivity ρ with decreasing temperature T reflect the Kondo lattice-heavy fermion behavior in CeRuSn₃ [8, 9]. However, both resistivity and Hall effect data reveal an absence of coherence effect which was argued to be due to the possible existence of atomic disorder [8, 9]. The dc magnetic susceptibility χ was found to show a large magnitude without any magnetic order above 1.7 K. On the other hand, ac $\chi(T)$ was found to show a sharp anomaly at $T \approx 0.5$ K and this was accompanied with a broad peak near 0.5 K in specific heat C_p/T versus T which Takayanagi *et al.* [9] suggested to be related to antiferromagnetic ordering or spin-glass transition.

In this contribution through the $\chi(T)$, $M(H)$, $C_p(T)$, $\rho(T, H)$, muon spin relaxation (μ SR) and inelastic neutron scattering (INS) investigations we show that there is no long range magnetic



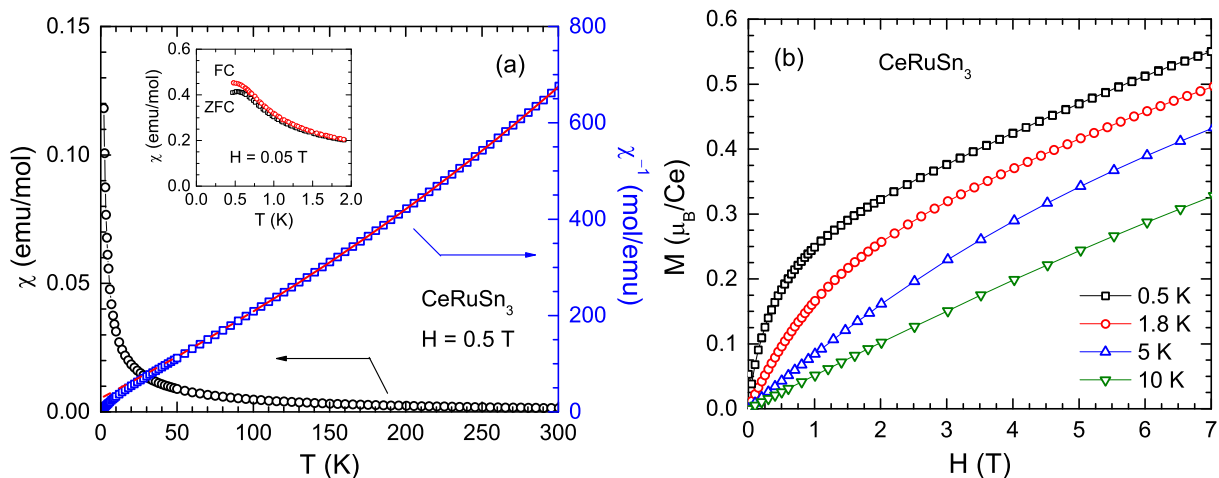


Figure 1. (a) Zero field cooled (ZFC) magnetic susceptibility χ of CeRuSn_3 as a function of temperature T and its inverse χ^{-1} for $2 \text{ K} \leq T \leq 300 \text{ K}$ measured in a magnetic field $H = 0.5 \text{ T}$. The solid line represents the fit by modified Curie-Weiss law for $100 \text{ K} \leq T \leq 300 \text{ K}$. Inset: ZFC and FC (field cooled) low- T $\chi(T)$ for $H = 0.05 \text{ T}$. (b) Isothermal magnetization M of CeRuSn_3 as a function of H measured at the indicated temperatures 0.5 K, 1.8 K, 5 K and 10 K.

order in CeRuSn_3 and a glassy spin-dynamics is favored. Recently, we found a ferromagnetic cluster spin-glass behavior in isostructural PrRhSn_3 [10] and a complex magnetic ground state in the Kondo lattice heavy fermion system CeRhSn_3 [11].

2. Experimental

The experimental details of sample synthesis and $\chi(T)$, $M(H)$, $C_p(T)$ and $\rho(T, H)$ measurements can be found in [11]. The muon spin relaxation experiment was performed using MuSR spectrometer at ISIS facility of the Rutherford Appleton Laboratory, Didcot, U.K. For μSR experiment the powdered sample of CeRuSn_3 was mounted on a high purity silver holder using diluted GE varnish that was covered with a thin silver foil. The sample mount was cooled in a dilution refrigerator to achieve the low temperature down to 84 mK. The inelastic neutron scattering experiment was performed with the HET time of flight spectrometer at ISIS. For INS experiment the powdered sample was filled in a thin Al-foil envelop ($40 \times 40 \times 0.5 \text{ mm}^3$) and mounted inside a top-loading closed cycle refrigerator (CCR).

3. Results and Discussion

The $\chi(T)$ of CeRuSn_3 and its inverse χ^{-1} measured in magnetic field $H = 0.5 \text{ T}$ are shown in figure 1(a). The zero field cooled (ZFC) and field cooled (FC) low- T $\chi(T)$ shown in inset exhibit an irreversibility that sets in at a temperature slightly above 0.6 K and ZFC χ shows a broad anomaly near 0.6 K. Further we see that the χ attains a value $\approx 0.4 \text{ emu/mol}$ which is rather large for a Kondo system, as also reported previously [8, 9]. At high- T the $\chi(T)$ follows modified Curie-Weiss behavior $\chi(T) = \chi_0 + C/(T - \theta_p)$. A fit of $\chi^{-1}(T)$ with this expression over $100 \text{ K} \leq T \leq 300 \text{ K}$ gives T -independent contribution to susceptibility $\chi_0 = -4.6(1) \times 10^{-4} \text{ emu/mol}$, Curie constant $C = 0.616(2) \text{ emu K/mole}$, and Weiss temperature $\theta_p = -17.2(3) \text{ K}$. The solid curve in figure 1(a) shows the fit of $\chi^{-1}(T)$ data with these fitting parameters. An effective moment $\mu_{\text{eff}} = 2.22(1) \mu_B$ is obtained from the value of C using $\mu_{\text{eff}} \approx \sqrt{8C} \mu_B$. The μ_{eff} obtained so is smaller than the expected value of $2.54 \mu_B/\text{Ce}$ for Ce^{3+} ions with $J = 5/2$.

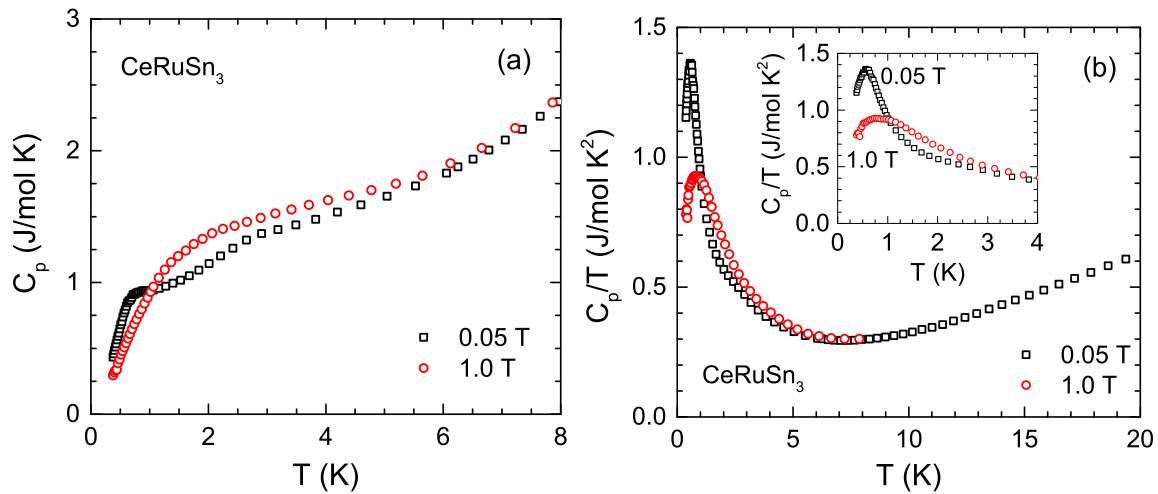


Figure 2. (a) Specific heat C_p of CeRuSn₃ as a function of temperature T for $0.38 \text{ K} \leq T \leq 8 \text{ K}$ measured in applied fields $H = 0.05 \text{ T}$ and 1.0 T . (b) C_p/T versus T plot for $0.38 \text{ K} \leq T \leq 20 \text{ K}$. Inset: Expanded view of C_p/T versus T plot for $T \leq 4 \text{ K}$.

The isothermal magnetization $M(H)$ data of CeRuSn₃ measured at selected temperatures of 0.5 K, 1.8 K, 5 K and 10 K are shown in figure 1(b). While at 10 K M is almost linear in H , at 1.8 K the $M(H)$ isotherm shows slight nonlinearity likely due to the presence of short range magnetic correlations. At 0.5 K the nonlinearity is even more pronounced. Further, the $M(H)$ isotherm at 0.5 K shows that the M attains a value of only $0.55 \mu_B$ at the highest measured field $H = 7 \text{ T}$. This value of M is much lower than the expected saturation value of $M_s = 2.14 \mu_B/\text{Ce}^{3+}$. The low value of M at 7 T could be due to the crystal field effect and/or due to the screening of moment by Kondo effect.

The $C_p(T)$ data of CeRuSn₃ measured in $H = 0.05 \text{ T}$ and 1.0 T for $0.38 \text{ K} \leq T \leq 20 \text{ K}$ are shown in figure 2. As shown in figure 2(a) the low- T $C_p(T)$ data ($H = 0.05 \text{ T}$) of CeRuSn₃ show a broad hump near 3 K (related to Kondo temperature T_K) and a rapid decrease below 0.6 K. The $C_p(T)$ data when plotted as C_p/T versus T as shown in figure 2(b) initially decreases with decreasing T down to about 7 K below which an increase is observed in C_p/T with decreasing T until it reaches a maximum near 0.6 K below which C_p/T starts decreasing again with decreasing T . The $C_p(T)$ data measured at $H = 1.0 \text{ T}$ show that the entropy associated with the peak in $C_p(T)/T$ is smeared out, and the peak becomes broader, moves towards the higher temperature side and peak height is reduced [inset of figure 2(b)]. The $C_p(T)/T$ data could be nicely fitted by $C_p/T = \gamma + \beta T^2$ and a fit over $10 \text{ K} \leq T \leq 15 \text{ K}$ yielded $\gamma = 212(2) \text{ mJ/mol K}^2$ and $\beta = 1.12(1) \text{ mJ/mol K}^4$. Since at lower T C_p/T shows an increase with decreasing T , $\gamma \geq 212(2) \text{ mJ/mol K}^2$ and reflects the heavy fermion behavior in CeRuSn₃. A comparison of γ values of CeRuSn₃ and LaRuSn₃ [$\gamma = 5.0(5) \text{ mJ/mol K}^2$] suggests the quasi-particle density of states renormalization factor due to $4f$ correlations in CeRuSn₃ to be ≈ 42 .

The $\rho(T)$ data of CeRuSn₃ measured in zero field for $2 \text{ K} \leq T \leq 350 \text{ K}$ are shown in figure 3. The T dependence of ρ reflects the Kondo lattice behavior. It is seen from figure 3(a) that the ρ increases with decreasing T with a broad maximum near 40 K and a minima around 20 K below which there is again an increase in ρ with decreasing T and peaks at 4 K. The origin of this 4 K anomaly in $\rho(T)$ which persists even at $H = 1.0 \text{ T}$ [upper inset of figure 3(a)] is not clear, but could be related to an onset of coherence among $4f$ -electrons. The T dependence of ρ is qualitatively similar to what has been reported previously, however no anomaly is reported near

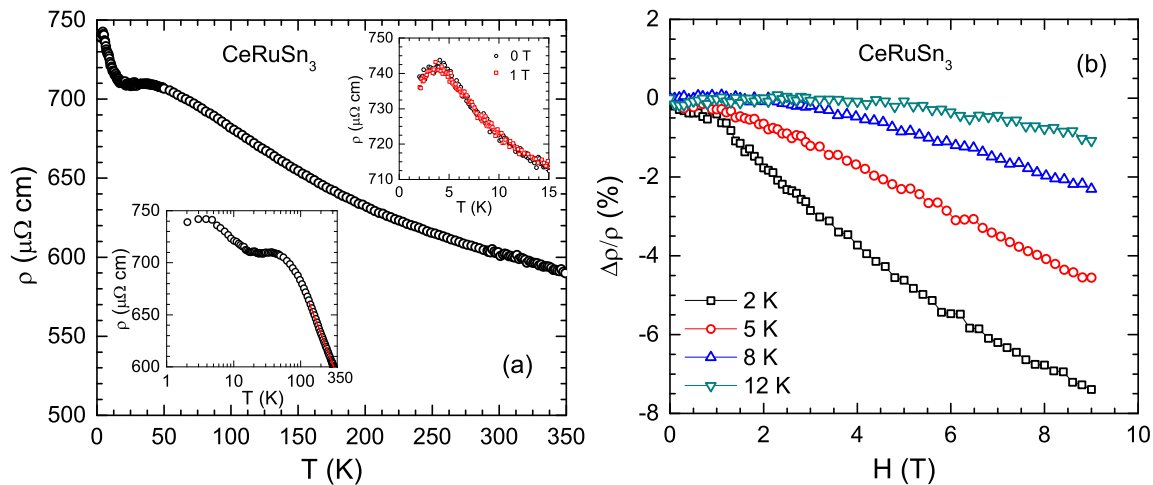


Figure 3. (a) Electrical resistivity ρ of CeRuSn_3 as a function of temperature T in $2 \text{ K} \leq T \leq 350 \text{ K}$ measured in applied field $H = 0$. Upper inset: Low- T $\rho(T)$ data at $H = 0$ and 1.0 T. Lower inset: $\rho(T)$ data plotted on a semi-logarithmic scale. The red solid line is a fit of $\rho(T)$ data by $\rho(T) = \rho_0 - c_K \ln T$ for $200 \text{ K} \leq T \leq 350 \text{ K}$. (b) ρ as a function of H , plotted as magnetoconductance $\Delta\rho(H)/\rho(0)$ for the indicated temperatures of 2, 5, 8 and 12 K.

4 K [8, 9]. The Kondo lattice behavior is quite clear from the semi-logarithmic plot of $\rho(T)$ in the lower inset of figure 3(a), where two linear regimes of logarithmic temperature dependences are clearly observed, one in low- T regime and another in high- T regime. We fitted the $\rho(T)$ data in high T regime by $\rho(T) = \rho_0 - c_K \ln T$, where ρ_0 is the spin-disorder resistivity and c_K is the Kondo coefficient. A fit of $\rho(T)$ data over $200 \text{ K} \leq T \leq 350 \text{ K}$ yields $\rho_0 = 1020(2) \mu\Omega \text{ cm}$ and the Kondo coefficient $c_K = 73.3 \mu\Omega \text{ cm}$. The fit is shown by solid red line in the lower inset of figure 3(a). The high- T $-\ln T$ behavior of $\rho(T)$ is a characteristic feature of Kondo system. While a low- T $-\ln T$ behavior arises from the Kondo scattering from CEF ground state, a high- T $-\ln T$ behavior represents the Kondo scattering from excited multiplet of $J = 5/2$. The observed behavior of the resistivity, two logarithmic regimes separated by a hump near 40 K, can be understood by the theoretical model of Cornut and Coqblin [12] which includes effect of CEF in the presence of Kondo effect.

The $\rho(H)$ data measured at different T are shown in figure 3(b) as magnetoconductance (MR) $\Delta\rho(H)/\rho(0) = [\rho(H) - \rho(0)]/\rho(0)$, where $\rho(H)$ is the resistivity measured at an applied field H . It is seen that the transverse MR ($i \perp H$) is negative up to the measured field of 9 T. The magnitude of MR depends on temperature and decreases with increasing T . At 2.0 K initially the negative MR increases slowly up to 1.2 T, above which there is an increase in slope of $\Delta\rho(H)/\rho(0)$ and eventually at 9 T the negative MR is about 7.5%. At 5 K no change in slope is observed near 1.2 T, thus the change in the slope of MR at 2.0 K seems to be related to the 4 K anomaly in $\rho(T)$ discussed above. The negative MR in paramagnetic state of CeRuSn_3 can be associated with the freezing out of spin-flip scattering due to Kondo interaction.

The zero field μSR asymmetry spectra at few representative temperatures between 0.2 K and 1.9 K are shown in figure 4. The μSR spectra show weak damping above 1 K and damping becomes stronger with decreasing T and a clear change in muon depolarization rates at $T \leq 0.6 \text{ K}$ can be inferred from μSR data in figures 4(a)–(d). The muon initial asymmetry is found to remain nearly constant (irrespective of temperature) down to 84 mK. Further, there is no clear sign of time oscillations of the asymmetry down to the lowest T in the μSR spectra. Both these observations indicate that within the μSR probing time scale CeRuSn_3 does not exhibit a

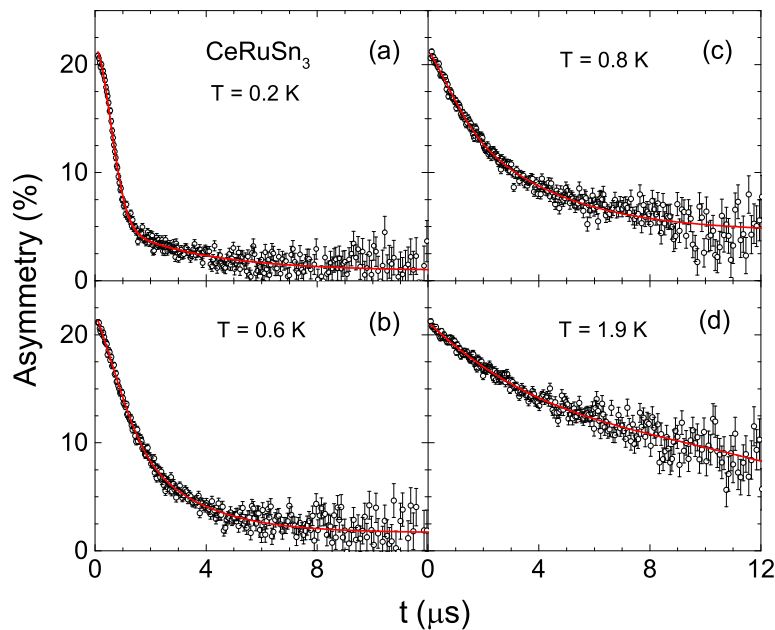


Figure 4. (a)–(d) Zero field muon-spin asymmetry function $G_z(t, H)$ versus time t μ SR spectra of CeRuSn_3 for few representative temperatures. The solid curves represent the fits of the data by the relaxation function given in equation (1).

clear sign of long range magnetic ordering. For a long range magnetically ordered system μ SR asymmetry spectra should show spontaneous time oscillations at the phase transition.

We analyzed the μ SR data of CeRuSn_3 taking into account both static and dynamic local fields at muon sites. While the static relaxation dominates at short time, at longer time the relaxation rate probes only the dynamic spin fluctuations. The μ SR data of CeRuSn_3 were analysed using the following form of the relaxation function,

$$G_z(t, H) = A_{01} \exp(-\lambda t) + A_{02} \exp\left(-\frac{\sigma^2 t^2}{2}\right) + BG, \quad (1)$$

where A_{01} and A_{02} are the initial asymmetries of the two components, and λ and σ are the depolarization rates. The first term in equation (1) (called Lorentzian form) accounts for the dynamic magnetic fluctuations, second term (called Gaussian form) accounts for isotropic Gaussian distribution of static fields and the third term is a constant background arising from muons stopping on the silver sample holder. The solid curves in figures 4(a)–(d) show the fits of μ SR data by this combination of Lorentzian and Gaussian decays. Our analysis of μ SR data reveals that the Gaussian contribution (static fluctuations) becomes sizable below 0.6 K and suggests a slowing down of spin fluctuations.

We also carried out analysis of μ SR data using Abragam functional form [13] which is applicable in an intermediate fluctuation range regime, i.e. in the limit between the slow (static, $\tau_c \sigma > 1$) and fast (dynamic, $\tau_c \sigma \ll 1$). The data between 0.084 K and 0.9 K could be fitted very well with this function and we found that $\tau_c \sigma \sim 1$ at 84 mK, which suggests that magnetic ground state in CeRuSn_3 is not fully static long range ordered, but short range ordered.

The inelastic neutron scattering response for the measurement using neutrons with incident energy $E_i = 23$ meV at 4.5 K is shown in figure 5. A broad excitation centered around 6–8 meV is inferred from the INS data in figure 5 that can be attributed to the crystal electric field (CEF)

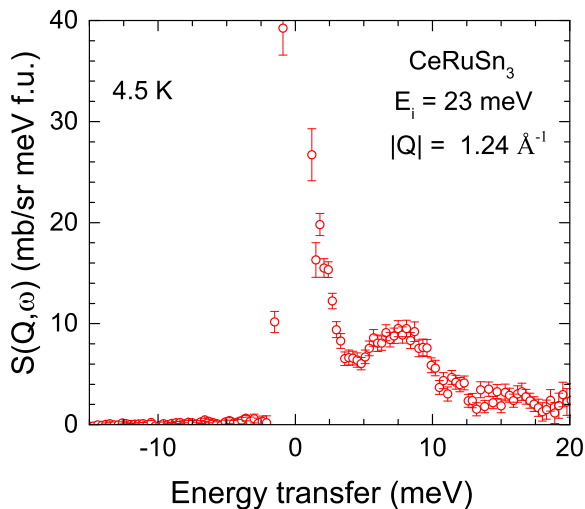


Figure 5. Q -integrated inelastic scattering intensity versus energy transfer of CeRuSn_3 at $|Q| = 1.24 \text{ \AA}^{-1}$ at 4.5 K for incident energy $E_i = 23 \text{ meV}$.

excitations of the Ce^{3+} . As there are two crystallographic Ce sites with cubic and tetragonal symmetries, we expect three CEF excitations (one from cubic and two from tetragonal Ce sites). However we see only a broad excitation near 6–8 meV, which indicates that the excitation from the two Ce sites have a similar energy scale. The analysis of INS data is underway.

4. Conclusions

The Kondo lattice and heavy fermion behaviors in CeRuSn_3 are confirmed from our $C_p(T)$ and $\rho(T)$ measurements. Both $\chi(T)$ and $C_p(T)$ reveal the reported anomaly at $T \approx 0.6 \text{ K} < T_K \approx 3.1 \text{ K}$. Observation of an irreversibility between the ZFC and FC $\chi(T)$ suggests that the anomaly is not related to an antiferromagnetic transition as is also inferred from the μSR data which does not show any spontaneous oscillations down to 84 mK to reveal a long range magnetic order. Short range ordering and glassy spin-dynamics seems apposite in CeRuSn_3 . The INS data show only a broad crystal electric field (CEF) excitation centered around 6–8 meV contrasting the expected three CEF excitations.

Acknowledgments

VKA, DTA and ADH acknowledge financial assistance from CMPC-STFC grant number CMPC-09108. AB thanks UJ and STFC for PDF funding. AMS thanks the SA-NRF (78832) and the URC of UJ for financial assistance.

References

- [1] Stewart G R 1984 *Rev. Mod. Phys.* **56** 755; Stewart G R 2001 *Rev. Mod. Phys.* **73** 797
- [2] Amato A 1997 *Rev. Mod. Phys.* **69** 1119
- [3] Riseborough P S 2000 *Adv. Phys.* **49** 257
- [4] von Löhneysen H, Rosch A, Vojta M and Woelfle P 2007 *Rev. Mod. Phys.* **79** 1015
- [5] Pfeleiderer C 2009 *Rev. Mod. Phys.* **81** 1551
- [6] Shaginyan V R, Amusia M Y, Msezane A Z and Popov K G 2010 *Phys. Reports* **492** 31
- [7] Eisenmann B and Schäfer H 1986 *J. Less-Common Metals* **123** 89
- [8] Fukuhara T, Sakamoto I, Sato H, Takayanagi S and Wada N 1989 *J. Phys.: Condens. Matter* **1** 7487
- [9] Takayanagi S, Fukuhara T, Sato H, Wada N and Yamada Y 1990 *Physica B* **165** & **166** 447
- [10] Anand V K, D. T. Adroja D T and Hillier A D 2012 *Phys. Rev. B* **85** 014418
- [11] Anand V K, Adroja D T, Hillier A D, Kockelmann W, Fraile A and Strydom A M 2011 *J. Phys.: Condens. Matter* **23** 276001
- [12] Cornut B and Coqblin B 1972 *Phys. Rev. B* **5** 4541
- [13] Keren A 1994 *Phys. Rev. B* **50** 10039